Author(s): Hinkkanen, Marko & Tuovinen, Toni & Harnefors, Lennart & Luomi, Jorma

Title: Analysis and design of a position observer with stator-resistance adaptation for PMSM drives

Year: 2010

Version: Post print

Please cite the original version:

Hinkkanen, Marko & Tuovinen, Toni & Harnefors, Lennart & Luomi, Jorma. 2010. Analysis and design of a position observer with stator-resistance adaptation for PMSM drives. 2010 XIX International Conference on Electrical Machines (ICEM). 6. ISBN 978-1-4244-4175-4 (electronic). DOI: 10.1109/icelmach.2010.5607900.

Analysis and Design of a Position Observer With Stator-Resistance Adaptation for PMSM Drives

Marko Hinkkanen*, Toni Tuovinen*, Lennart Harnefors†, and Jorma Luomi*
*Aalto University School of Science and Technology
Department of Electrical Engineering, P.O. Box 13000, FI-00076 Aalto, Finland
†ABB Power Systems, PSDC/DCTU, SE-77180 Ludvika, Sweden

***Abstract*—This paper deals with reduced-order observers with stator-resistance adaptation for motion-sensorless permanent-magnet synchronous motor drives. An analytical solution for the stabilizing observer gain and stability conditions for the stator-resistance adaptation are derived. The proposed observer design is experimentally tested using a 2.2-kW motor drive; stable operation at very low speeds under different loading conditions is demonstrated.**

***Index Terms*—Observer, stability conditions, sensorless, stator resistance estimation.**

I. Introduction

Motion-sensorless permanent-magnet synchronous motor (PMSM) drives may have an unstable operating region at low speeds. Since the back electromotive force (EMF) is proportional to the rotational speed of the motor, parameter errors have a relatively high effect on the accuracy of the estimated back EMF at low speeds [1], [2]. Improper observer gain selections may cause unstable operation of the drive even if the parameters are accurately known [3], [4].

In practice, the stator resistance varies with the winding temperature during the operation of the motor. The stator resistance can be estimated by injecting a test signal into the stator winding, or by using the fundamental excitation in combination with a machine model. For PMSMs, a dc-current signal has been used for identifying the stator resistance in [5]. A combination of steady-state equations and the response to an alternating-current signal has been used in [6]. In [7], [1], a model-reference adaptive system (MRAS) is applied for on-line stator-resistance estimation in order to improve the sensorless control. Usually, an in-depth stability analysis of these methods is omitted since the resulting closed-loop systems become very complicated.

In this paper, a reduced-order position observer is augmented with stator-resistance adaptation, based on the fundamental excitation, and analytical stability conditions and design rules are derived for the augmented observer. Based on these stability conditions, an easy-to-tune observer design is proposed. The proposed design is very simple, and it results in a robust and well-damped closed-loop system. The performance of the proposed observer design is evaluated using laboratory experiments with a 2.2-kW PMSM drive.

II. PMSM Model

Real space vectors will be used throughout the paper. Space vectors will be denoted by boldface lowercase letters and matrices by boldface uppercase letters. The matrix transpose will be marked with the superscript T. The identity matrix and the orthogonal rotation matrix are defined as

$$\mathbf{I} = \begin{bmatrix} 1 & 0 \\ 0 & 1 \end{bmatrix}, \quad \mathbf{J} = \begin{bmatrix} 0 & -1 \\ 1 & 0 \end{bmatrix} \tag{1}$$

respectively. Since $\mathbf{J}$ corresponds to the imaginary unit j, the notation is very similar to that obtained for complex space vectors.

To simplify the analysis in the following sections, the PMSM model will be expressed in the *estimated* rotor reference frame, whose d axis is aligned at $\hat{\vartheta}_\mathrm{m}$ with respect to the stator reference frame. The voltage and flux equations are

$$\frac{\mathrm{d}\boldsymbol{\psi}_\mathrm{s}}{\mathrm{d}t} + \hat{\omega}_\mathrm{m}\mathbf{J}\boldsymbol{\psi}_\mathrm{s} = \boldsymbol{u}_\mathrm{s} - R_\mathrm{s}\boldsymbol{i}_\mathrm{s} \tag{2a}$$

$$\boldsymbol{\psi}_\mathrm{s} = \boldsymbol{L}\boldsymbol{i}_\mathrm{s} + \boldsymbol{\psi}_\mathrm{pm} \tag{2b}$$

where $\boldsymbol{u}_\mathrm{s} = [u_\mathrm{d}, u_\mathrm{q}]^\mathrm{T}$ is the stator voltage vector, $\boldsymbol{i}_\mathrm{s} = [i_\mathrm{d}, i_\mathrm{q}]^\mathrm{T}$ the stator current vector, R_s the stator resistance, and $\hat{\omega}_\mathrm{m} = \mathrm{d}\hat{\vartheta}_\mathrm{m}/\mathrm{d}t$ is the angular speed of the reference frame. The stator inductance and the permanent-magnet flux vector are

$$\boldsymbol{L} = \mathrm{e}^{-\tilde{\vartheta}_\mathrm{m}\mathbf{J}} \begin{bmatrix} L_\mathrm{d} & 0 \\ 0 & L_\mathrm{q} \end{bmatrix} \mathrm{e}^{\tilde{\vartheta}_\mathrm{m}\mathbf{J}}, \quad \boldsymbol{\psi}_\mathrm{pm} = \mathrm{e}^{-\tilde{\vartheta}_\mathrm{m}\mathbf{J}} \begin{bmatrix} \psi_\mathrm{pm} \\ 0 \end{bmatrix} \tag{3}$$

respectively, where $\tilde{\vartheta}_\mathrm{m} = \hat{\vartheta}_\mathrm{m} - \vartheta_\mathrm{m}$. The electrical position of the permanent-magnet flux is ϑ_m and the angular speed of the rotor is $\omega_\mathrm{m} = \mathrm{d}\vartheta_\mathrm{m}/\mathrm{d}t$.

In the following, the back EMF induced by the permanent-magnet flux,

$$\boldsymbol{e} = \frac{\mathrm{d}\boldsymbol{\psi}_\mathrm{pm}}{\mathrm{d}t} + \hat{\omega}_\mathrm{m}\mathbf{J}\boldsymbol{\psi}_\mathrm{pm} \tag{4a}$$

will be used to formulate the rotor position observer. Based on (2), this back EMF can be expressed as

$$\boldsymbol{e} = \boldsymbol{u}_\mathrm{s} - R_\mathrm{s}\boldsymbol{i}_\mathrm{s} - \frac{\mathrm{d}}{\mathrm{d}t}\left(\boldsymbol{L}\boldsymbol{i}_\mathrm{s}\right) - \hat{\omega}_\mathrm{m}\mathbf{J}\boldsymbol{L}\boldsymbol{i}_\mathrm{s} \tag{4b}$$

III. Rotor-Position Observer

To avoid forbiddingly complicated equations, which would prevent analytical results from being derived, accurate parameter estimates L_d, L_q, and ψ_pm are assumed, with the exception of the stator-resistance estimate $\hat{R}_\mathrm{s}$. Without loss of generality, the observer in estimated rotor coordinates is considered. Since

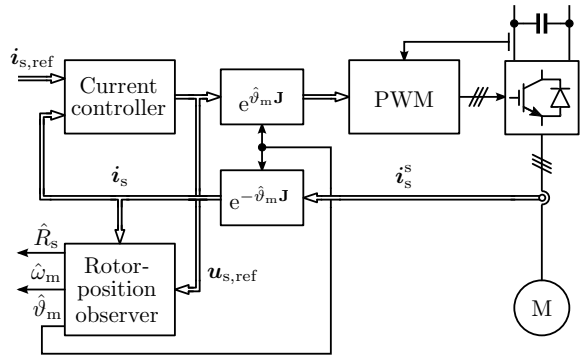

Fig. 1. Motion-sensorless rotor-oriented controller. The observer is implemented in the estimated rotor coordinates.

the rotor-position estimation error is unknown, the inductance matrix and permanent-magnet-flux vector estimates are

$$\hat{\boldsymbol{L}} = \begin{bmatrix} L_\mathrm{d} & 0 \\ 0 & L_\mathrm{q} \end{bmatrix}, \quad \hat{\boldsymbol{\psi}}_\mathrm{pm} = \begin{bmatrix} \psi_\mathrm{pm} \\ 0 \end{bmatrix} \tag{5}$$

respectively. A typical rotor-oriented control system is depicted in Fig. 1, where the rotor-position estimate $\hat{\vartheta}_\mathrm{m}$ is calculated in estimated rotor coordinates.

A. Observer Structure

Based on (4), two estimates for the back EMF induced by the permanent-magnet flux can be calculated:

$$\hat{\boldsymbol{e}} = \hat{\omega}_\mathrm{m} \mathbf{J} \hat{\boldsymbol{\psi}}_\mathrm{pm} \tag{6a}$$

$$\boldsymbol{e}' = \boldsymbol{u}_\mathrm{s} - \hat{R}_\mathrm{s} \boldsymbol{i}_\mathrm{s} - \hat{\boldsymbol{L}} \frac{\mathrm{d}\boldsymbol{i}_\mathrm{s}}{\mathrm{d}t} - \hat{\omega}_\mathrm{m} \mathbf{J} \hat{\boldsymbol{L}} \boldsymbol{i}_\mathrm{s} \tag{6b}$$

It is worth noticing that $\mathrm{d}\hat{\boldsymbol{\psi}}_\mathrm{pm}/\mathrm{d}t = 0$ in (6a) since constant ψ_pm is assumed. Since the current derivative $\mathrm{d}\boldsymbol{i}_\mathrm{s}/\mathrm{d}t$ is known (either measured or calculated in the discrete observer using the sample from the previous time step), the rotor speed estimate $\hat{\omega}_\mathrm{m}$ can be evaluated using an algebraic relation[1]. Using (6), an observer can be formulated:

$$\boldsymbol{k}^\mathrm{T} (\hat{\boldsymbol{e}} - \boldsymbol{e}') = 0 \tag{7}$$

where $\boldsymbol{k}$ is a gain vector. It can be seen from (7) that the magnitude of the gain vector is irrelevant: $\boldsymbol{k} = [g, 1]^\mathrm{T}$ can be selected without loss of generality. From (7) and $\hat{\omega}_\mathrm{m} = \mathrm{d}\hat{\vartheta}_\mathrm{m}/\mathrm{d}t$, the differential equation for the rotor position estimate can be solved:

$$\frac{\mathrm{d}\hat{\vartheta}_\mathrm{m}}{\mathrm{d}t} = \frac{\boldsymbol{k}^\mathrm{T} \left(\boldsymbol{u}_\mathrm{s} - \hat{R}_\mathrm{s} \boldsymbol{i}_\mathrm{s} - \hat{\boldsymbol{L}} \dfrac{\mathrm{d}\boldsymbol{i}_\mathrm{s}}{\mathrm{d}t} \right)}{\boldsymbol{k}^\mathrm{T} \mathbf{J} (\hat{\boldsymbol{\psi}}_\mathrm{pm} + \hat{\boldsymbol{L}} \boldsymbol{i}_\mathrm{s})} = \hat{\omega}_\mathrm{m} \tag{8}$$

or expressed using components:

$$\frac{\mathrm{d}\hat{\vartheta}_\mathrm{m}}{\mathrm{d}t} = \frac{u_\mathrm{q} - \hat{R}_\mathrm{s} i_\mathrm{q} - L_\mathrm{q} \frac{\mathrm{d}i_\mathrm{q}}{\mathrm{d}t} + g(u_\mathrm{d} - \hat{R}_\mathrm{s} i_\mathrm{d} - L_\mathrm{d} \frac{\mathrm{d}i_\mathrm{d}}{\mathrm{d}t})}{\psi_\mathrm{pm} + L_\mathrm{d} i_\mathrm{d} - g L_\mathrm{q} i_\mathrm{q}} \tag{9}$$

Choosing $g = 0$ leads to the pure voltage model. Naturally, the same observer (8) would be obtained by using the back EMF induced by the stator flux in the derivation. The rotor-position observer is of the first order, and there is only one gain, g, to select.

[1]If knowledge of $\mathrm{d}\boldsymbol{i}_\mathrm{s}/\mathrm{d}t$ were not available, a full-order observer would be needed.

B. Stabilizing Observer Gain

As shown in Appendix A, the closed-loop system consisting of (2) and (9) is locally stable if the gain is given by

$$g = \frac{\beta - \alpha/\hat{\omega}_\mathrm{m}}{\beta\alpha/\hat{\omega}_\mathrm{m} + 1} \tag{10}$$

where $\alpha > 0$ corresponds to the bandwidth of the position estimation and

$$\beta = \frac{(L_\mathrm{d} - L_\mathrm{q}) i_\mathrm{q}}{\psi_\mathrm{pm} + (L_\mathrm{d} - L_\mathrm{q}) i_\mathrm{d}} \tag{11}$$

As a special case, (11) reduces to $\beta = 0$ for non-salient PMSMs.

It is necessary that the bandwidth α depends on the operating point. For $\hat{\omega}_\mathrm{m} = 0$, $\alpha = 0$ has to be selected to avoid division by zero, giving only marginal stability for zero frequency. Furthermore, the denominator of the gain (10) should be nonzero:

$$\alpha \neq -\hat{\omega}_\mathrm{m}/\beta \tag{12}$$

For typical salient and non-salient PMSMs, the bandwidth can be selected as

$$\alpha = \lambda |\hat{\omega}_\mathrm{m}| \tag{13}$$

where λ is a positive constant that should be smaller than any expected value for $1/|\beta|$. This selection corresponds to the gain

$$g = \frac{\beta - \lambda \operatorname{sign}(\hat{\omega}_\mathrm{m})}{\beta\lambda \operatorname{sign}(\hat{\omega}_\mathrm{m}) + 1} \tag{14}$$

It is to be noted, however, that if the saliency ratio is large while the permanent-magnet flux is small, the condition $\lambda < 1/|\beta|$ cannot always be fulfilled. As a worst-case example, a synchronous reluctance motor—for which $\beta = i_\mathrm{q}/i_\mathrm{d}$ holds—can be considered. If the current component i_d is kept constant, $1/\beta$ becomes close to zero at high values of i_q. Therefore, a very small value for λ should be selected, resulting in the problems typical to the pure voltage model. It seems that a slightly more complex observer structure is necessary for this kind of machines [8].

C. Conventional Designs for Non-Salient PMSMs

In [9], a similar observer was proposed for non-salient PMSMs. The gain was selected as

$$g = -\lambda \operatorname{sign}(\hat{\omega}_\mathrm{m}) \tag{15}$$

where λ is a positive constant. According to (14) with $\beta = 0$, this selection results in the stable system having the bandwidth of $\alpha = \lambda |\hat{\omega}_\mathrm{m}|$.

In [2], the observer was made insensitive to the stator resistance at low speeds by using the observer gain

$$g = -i_\mathrm{q}/i_\mathrm{d} \tag{16}$$

This gain removes the stator-resistance estimate from the observer (9). In order to stabilize the observer, the current component i_d was controlled according to

$$i_\mathrm{d} = i_\mathrm{q}\,\mathrm{sign}(\hat{\omega}_\mathrm{m})/\lambda \tag{17}$$

The observer gain (16) together with the control law (17) leads to the stable system having the position-estimation bandwidth $\alpha = \lambda|\hat{\omega}_\mathrm{m}|$.

IV. Stator-Resistance Adaptation

Since (7) is used for position estimation, the component of the back-EMF estimation error is zero in the direction of the gain vector. The component perpendicular to $\boldsymbol{k}$, however, can be used for the stator-resistance adaptation,

$$\frac{\mathrm{d}\hat{R}_\mathrm{s}}{\mathrm{d}t} = \gamma \boldsymbol{k}^\mathrm{T}\mathbf{J}(\hat{\boldsymbol{e}} - \boldsymbol{e}') \tag{18}$$

where γ is a gain. The stability conditions for the position observer (9) augmented with (18) are derived in Appendix B. These conditions are fulfilled by choosing

$$\gamma = \begin{cases} L, & \text{if } 0 < L < \gamma'\,\mathrm{sign}(x) \\ L, & \text{if } \gamma'\,\mathrm{sign}(x) < L < 0 \\ \gamma'\,\mathrm{sign}(x), & \text{otherwise} \end{cases} \tag{19}$$

where γ' is a positive design parameter. The sign of the gain γ depends on

$$x = g(\alpha i_\mathrm{q} - \hat{\omega}_\mathrm{m} i_\mathrm{d}) - \alpha i_\mathrm{d} - \hat{\omega}_\mathrm{m} i_\mathrm{q} \tag{20}$$

Furthermore, the limiting value is

$$L = -r\frac{\alpha\hat{\omega}_\mathrm{m}}{g(\alpha i_\mathrm{d} + \hat{\omega}_\mathrm{m} i_\mathrm{q}) + \alpha i_\mathrm{q} - \hat{\omega}_\mathrm{m} i_\mathrm{d}} \tag{21}$$

where the parameter $0 < r < 1$ affects the stability margin of the system; choosing $r = 1$ would lead to a marginally stable system (in the operating points where γ is determined by L).

The adaptation should be disabled in the vicinity of no-load operation and at higher stator frequencies due to poor signal-to-noise ratio (which is a fundamental property common to all stator-resistance adaptation methods based only on the fundamental-wave excitation). Hence, parameter γ' in (19) can be selected as

$$\gamma' = \begin{cases} \gamma''\left(1 - \frac{|\hat{\omega}_\mathrm{m}|}{\omega_\Delta}\right) i_\mathrm{s}, & \text{if } i_\mathrm{s} > i_\Delta \text{ and } |\hat{\omega}_\mathrm{m}| < \omega_\Delta \\ 0, & \text{otherwise} \end{cases} \tag{22}$$

where γ'' is a positive constant, ω_Δ is the transition frequency, and

$$i_\mathrm{s} = \sqrt{i_\mathrm{d}^2 + i_\mathrm{q}^2} \tag{23}$$

is the magnitude of the stator-current vector.

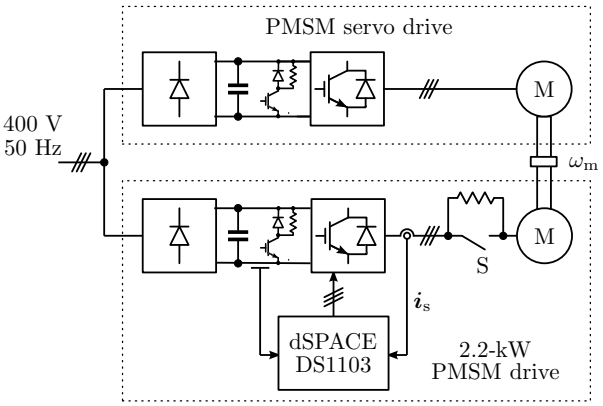

Fig. 2. Experimental setup. The stator currents and the DC-link voltage are used as feedback signals. Mechanical load is provided by a servo drive. The rotor speed ω_m is measured for monitoring purposes. Three-phase switch S is in the closed position, except in the experiment shown in Fig. 5.

V. Experimental Setup and Parameters

The operation of the proposed observer and stator-resistance adaptation was investigated experimentally using the setup shown in Fig. 2. The motion-sensorless control system was implemented in a dSPACE DS1103 PPC/DSP board. A 2.2-kW six-pole PMSM is fed by a frequency converter that is controlled by the DS1103 board. The rated values of the PMSM are: speed 1500 r/min; frequency 75 Hz; line-to-line rms voltage 370 V; rms current 4.3 A; and torque 14 Nm. The base values for angular speed, voltage, and current are defined as $2\pi \cdot 75$ rad/s, $\sqrt{2/3} \cdot 370$ V, and $\sqrt{2} \cdot 4.3$ A, respectively.

A servo PMSM is used as a loading machine. The rotor speed ω_m and position ϑ_m are measured using an incremental encoder for monitoring purposes. The total moment of inertia of the experimental setup is 0.015 kgm^2 (2.2 times the inertia of the 2.2-kW PMSM rotor).

The stator resistance of the 2.2-kW PMSM is approximately 3.3 Ω at room temperature. Additional 1-Ω resistors were added between the frequency converter and the PMSM. The resistance can be changed stepwise by opening or closing a manually operated three-phase switch (S) connected in parallel with the resistors. Unless otherwise noted, switch S is in the closed position.

The block diagram of the motion-sensorless control system implemented in the DS1103 board is shown in Fig. 1. The stator currents and the DC-link voltage are measured, and the reference voltage obtained from the current controller is used for the observer. The sampling is synchronized to the modulation, and both the switching frequency and the sampling frequency are 5 kHz. A simple current feedforward compensation for dead times and power device voltage drops is applied. The control system shown in Fig. 1 is augmented with a speed controller, whose feedback signal is the speed estimate $\hat{\omega}_\mathrm{m}$ obtained from the proposed observer. The bandwidth of this PI speed controller, including active damping [10], is 0.08 p.u. The estimate of the per-unit electromagnetic torque is evaluated as $\hat{T}_\mathrm{e} = \psi_\mathrm{pm} i_\mathrm{q} + (L_\mathrm{d} - L_\mathrm{q}) i_\mathrm{d} i_\mathrm{q}$.

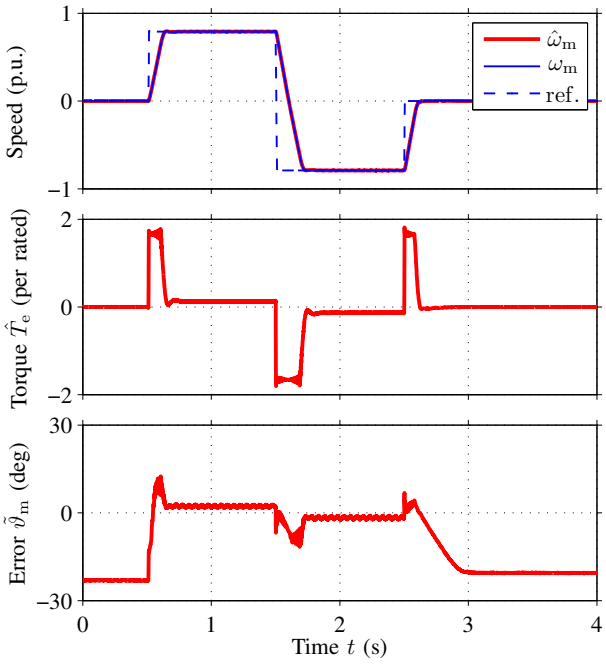

Fig. 3. Experimental results showing speed-reference steps (0 → 1200 rpm → −1200 rpm → 0) at no load.

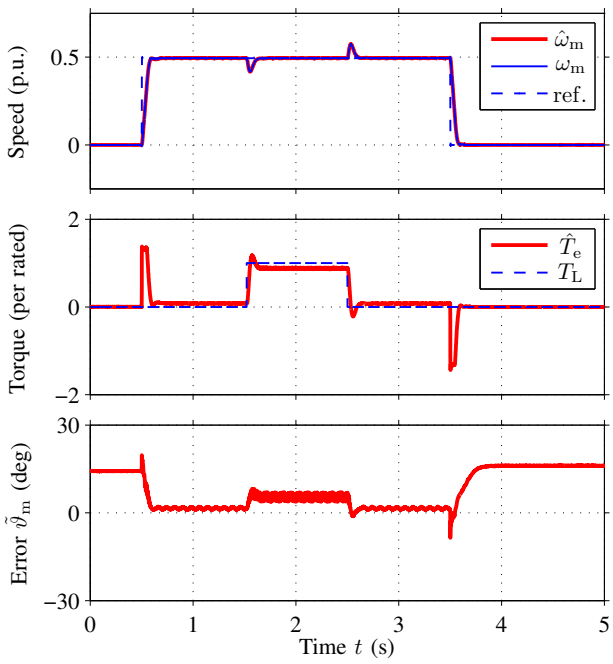

Fig. 4. Experimental results showing speed reference steps (0 → 750 rpm → 0). Rated load torque step is applied at t = 1.5 s and removed at t = 2.5 s. T_L shown in the second subplot is the torque reference of the loading drive.

The proposed observer was implemented in the estimated rotor coordinates using (9) and (18). The per-unit parameters used in the experiments are: $L_\mathrm{d} = 0.33$ p.u.; $L_\mathrm{q} = 0.45$ p.u.; and $\psi_\mathrm{pm} = 0.895$ p.u. The observer gain in (14) is determined by $\lambda = 0.5$. The parameters needed for the stator-resistance adaptation are: $r = 0.1$ in (21) and $\gamma'' = 0.01$ p.u., $\omega_\Delta = 0.25$ p.u., and $i_\Delta = 0.2$ p.u. in (22).

VI. Experimental Results

Fig. 3 shows results of medium-speed no-load operation. The speed reference was stepped from 0 to 1200 rpm, then to −1200 rpm and finally back to 0. According to (22), the stator-resistance adaptation was only active in the beginning of the acceleration and at the end of the deceleration. Even though there is an initial error of approximately 20 electrical degrees in the rotor position estimate, it can be seen that the position estimate quickly converges close to the actual position in the beginning of the acceleration. The position error increases slightly at the end of the deceleration ($t > 2.5$ s) since the stator current, voltage and frequency approach zero and, therefore, there is no information available on the position. However, it is worth noticing that the position estimate remains stable at zero speed and the drive could be accelerated again.

Fig. 4 depicts a rated load torque step and its removal at the speed of 750 rpm. It can be seen that the response against these load-torque disturbances is well damped.

Fig. 5 shows the stepwise change in the stator resistance (as seen by the frequency converter). Initially, three-phase switch S, cf. Fig. 2, was in the closed position. The speed reference was kept at 45 rpm. A rated-load torque step was applied at $t = 2$ s. Switch S was opened at $t = 5.5$ s, causing 0.02-p.u. increase (corresponding to 30%) in the actual stator resistance. It can be seen that the stator-resistance estimate tracks the change in the actual stator resistance.

Fig. 6 shows load-torque steps when the speed reference was kept at 30 rpm. The load torque was stepped to the rated value at $t = 2.5$ s, reversed at $t = 7.5$ s, and removed at $t = 12.5$ s. It can be seen that the proposed observer behaves well in torque transients.

Results of a slow speed reversals are shown in Fig. 7. A rated-load torque step was applied at $t = 2$ s. The speed reference was slowly ramped from 150 rpm to −150 rpm and back to 150 rpm. During the sequence, the drive operates in the motoring and regenerating modes. In the vicinity of zero frequency, the rotor-position estimate begins to deviate from the actual position but the system remains stable. Without the stator-resistance adaptation, a very accurate stator-resistance estimate would be needed since the frequency remains in the vicinity of zero for a long time.

VII. Conclusions

In this paper, analytical stability conditions and design rules are derived for the reduced-order position observer augmented with the stator-resistance adaptation. A stabilizing gain for the position observer is presented. A stator-resistance adaptation law is proposed, and stability conditions are derived for the system augmented with the resistance adaptation. Based on these stability conditions, an easy-to-tune observer design is proposed. The proposed design is very simple, and it results in a robust and well-damped closed-loop system. The performance of the proposed observer design was evaluated using

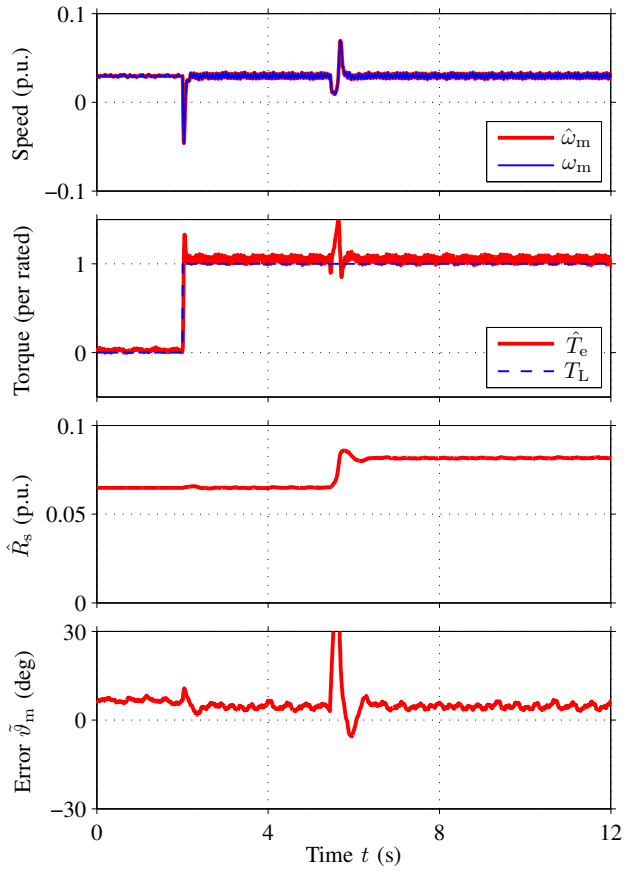

Fig. 5. Experimental results showing the stepwise increase of 1 Ω in the actual stator resistance at $t = 5.5$ s. Speed reference is kept at 45 rpm and a rated load torque is applied at $t = 2$ s.

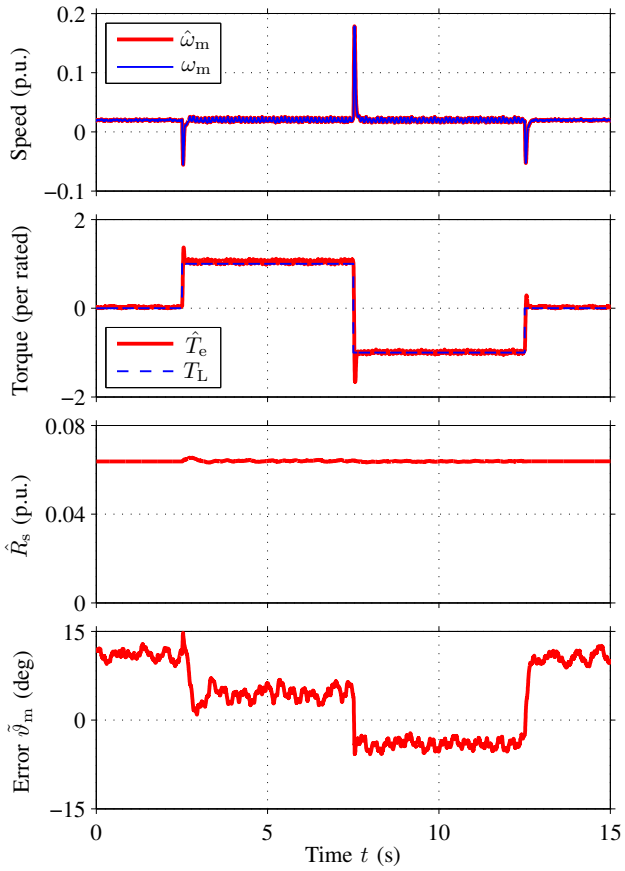

Fig. 6. Experimental results showing load-torque steps (0 → rated → negative rated → 0) when the speed reference is kept at 30 rpm.

laboratory experiments with a 2.2-kW PMSM drive. Stable operation at very low speeds under different loading conditions was demonstrated. Furthermore, it was experimentally verified that the stator-resistance estimate can track stepwise changes in the actual resistance.

Appendix A
Derivation of a Stabilizing Observer Gain

From (2) and (9), the nonlinear dynamics of the estimation error are obtained:

$$\frac{\mathrm{d}\tilde{\vartheta}_\mathrm{m}}{\mathrm{d}t} = -\frac{\boldsymbol{k}^\mathrm{T}\left[\omega_\mathrm{m}\mathbf{J}(\tilde{\boldsymbol{\psi}}_\mathrm{pm} + \tilde{\boldsymbol{L}}\boldsymbol{i}_\mathrm{s}) + \tilde{\boldsymbol{L}}\frac{\mathrm{d}\boldsymbol{i}_\mathrm{s}}{\mathrm{d}t} + \tilde{R}_\mathrm{s}\boldsymbol{i}_\mathrm{s}\right]}{\boldsymbol{k}^\mathrm{T}\left[\mathbf{J}(\tilde{\boldsymbol{\psi}}_\mathrm{pm} + \tilde{\boldsymbol{L}}\boldsymbol{i}_\mathrm{s}) + \frac{\mathrm{d}\tilde{\boldsymbol{L}}}{\mathrm{d}\tilde{\vartheta}_\mathrm{m}}\boldsymbol{i}_\mathrm{s} + \frac{\mathrm{d}\tilde{\boldsymbol{\psi}}_\mathrm{pm}}{\mathrm{d}\tilde{\vartheta}_\mathrm{m}}\right]} \tag{24}$$

where $\tilde{\vartheta}_\mathrm{m} = \hat{\vartheta}_\mathrm{m} - \vartheta_\mathrm{m}$ is the estimation error of the rotor position, $\tilde{\boldsymbol{\psi}}_\mathrm{pm} = \hat{\boldsymbol{\psi}}_\mathrm{pm} - \boldsymbol{\psi}_\mathrm{pm}$ is error in the permanent-magnet flux vector, $\tilde{\boldsymbol{L}} = \hat{\boldsymbol{L}} - \boldsymbol{L}$ is the error in the inductance matrix, and $\tilde{R}_\mathrm{s} = \hat{R}_\mathrm{s} - R_\mathrm{s}$ is the error in the stator resistance estimate. It is worth noticing that the errors $\tilde{\boldsymbol{\psi}}_\mathrm{pm}$ and $\tilde{\boldsymbol{L}}$ originate only due to the angle error $\tilde{\vartheta}_\mathrm{m}$ (since accurate parameter estimates are assumed).

The local stability of the system (24) can be studied via small-signal linearization. The operating-point quantities will be marked by the subscript 0. The operating-point inductance matrix and permanent-magnet flux are

$$\boldsymbol{L}_0 = \begin{bmatrix} L_\mathrm{d} & 0 \\ 0 & L_\mathrm{q} \end{bmatrix}, \quad \boldsymbol{\psi}_\mathrm{pm0} = \begin{bmatrix} \psi_\mathrm{pm} \\ 0 \end{bmatrix} \tag{25}$$

respectively. To simplify the notation, a fictitious flux is defined

$$\begin{aligned} \boldsymbol{\psi}_0 &= \boldsymbol{\psi}_\mathrm{pm0} + (\boldsymbol{L}_0 + \mathbf{J}\boldsymbol{L}_0\mathbf{J})\boldsymbol{i}_\mathrm{s0} \\ &= \begin{bmatrix} \psi_\mathrm{pm} + (L_\mathrm{d} - L_\mathrm{q})i_\mathrm{d0} \\ -(L_\mathrm{d} - L_\mathrm{q})i_\mathrm{q0} \end{bmatrix} \end{aligned} \tag{26}$$

When $\tilde{R}_\mathrm{s} = 0$ and $(\mathrm{d}\boldsymbol{i}_\mathrm{s}/\mathrm{d}t)_0 = 0$ are assumed, the linearization results in

$$\frac{\mathrm{d}\tilde{\vartheta}_\mathrm{m}}{\mathrm{d}t} = -\alpha_0\tilde{\vartheta}_\mathrm{m} \tag{27}$$

where the coefficient

$$\alpha_0 = -\frac{\omega_\mathrm{m0}\boldsymbol{k}_0^\mathrm{T}\boldsymbol{\psi}_0}{\boldsymbol{k}_0^\mathrm{T}\mathbf{J}\boldsymbol{\psi}_0} = \frac{\omega_\mathrm{m0}(\beta_0 - g_0)}{1 + \beta_0 g_0} \tag{28}$$

corresponds to the bandwidth of the position estimation. The nonlinear closed-loop system (24) is locally stable if $\alpha_0 > 0$. From (28), the stabilizing gain can be solved:

$$g_0 = \frac{\beta_0\omega_\mathrm{m0} - \alpha_0}{\beta_0\alpha_0 + \omega_\mathrm{m0}} \tag{29}$$

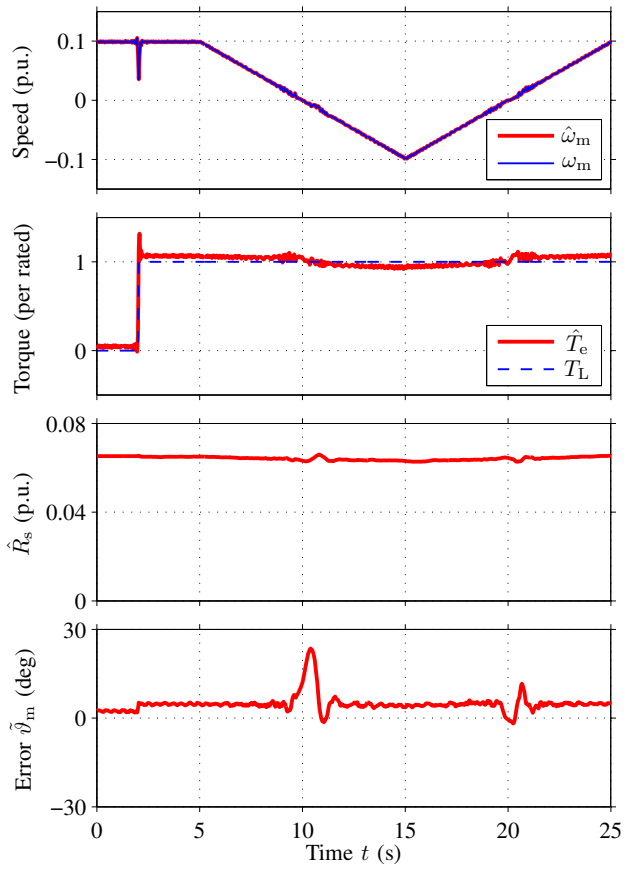

Fig. 7. Experimental results showing slow speed reversals (150 rpm $\rightarrow -150$ rpm $\rightarrow$ 150 rpm) when the rated load torque is applied.

The bandwidth should be selected so that the denominator in (29) is nonzero:

$$\alpha_0 \neq -\omega_{\mathrm{m}0}/\beta_0 \tag{30}$$

Appendix B
Stability of Stator-Resistance Adaptation

Assuming constant R_s and the stator-resistance adaptation law (18), the nonlinear dynamics of the stator resistance estimation error become

$$\begin{aligned}\frac{\mathrm{d}\tilde{R}_\mathrm{s}}{\mathrm{d}t} = \gamma \boldsymbol{k}^\mathrm{T}\mathbf{J}\Bigg[\tilde{\boldsymbol{L}}\frac{\mathrm{d}\boldsymbol{i}_\mathrm{s}}{\mathrm{d}t} + \tilde{\omega}_\mathrm{m}\left(\frac{\mathrm{d}\tilde{\boldsymbol{L}}}{\mathrm{d}\vartheta_\mathrm{m}}\boldsymbol{i}_\mathrm{s} + \frac{\mathrm{d}\tilde{\boldsymbol{\psi}}_\mathrm{pm}}{\mathrm{d}\vartheta_\mathrm{m}}\right) \\ + (\omega_\mathrm{m} + \tilde{\omega}_\mathrm{m})\mathbf{J}(\tilde{\boldsymbol{L}}\boldsymbol{i}_\mathrm{s} + \tilde{\boldsymbol{\psi}}_\mathrm{pm}) + \tilde{R}_\mathrm{s}\boldsymbol{i}_\mathrm{s}\Bigg]\end{aligned} \tag{31}$$

The closed-loop system consisting of (24) and (31) can be linearized:

$$\frac{\mathrm{d}\tilde{\vartheta}_\mathrm{m}}{\mathrm{d}t} = -\alpha_0\tilde{\vartheta}_\mathrm{m} - \frac{\boldsymbol{k}_0^\mathrm{T}\boldsymbol{i}_{\mathrm{s}0}}{\boldsymbol{k}_0^\mathrm{T}\mathbf{J}\boldsymbol{\psi}_0}\tilde{R}_\mathrm{s} \tag{32a}$$

$$\begin{aligned}\frac{\mathrm{d}\tilde{R}_\mathrm{s}}{\mathrm{d}t} &= \gamma_0\boldsymbol{k}_0^\mathrm{T}\left(\alpha_0\mathbf{I} - \omega_{\mathrm{m}0}\mathbf{J}\right)\boldsymbol{\psi}_0\tilde{\vartheta}_\mathrm{m} \\ &\quad - \gamma_0\frac{\boldsymbol{k}_0^\mathrm{T}\left(\alpha_0\mathbf{I} - \omega_{\mathrm{m}0}\mathbf{J}\right)\boldsymbol{i}_{\mathrm{s}0}}{\omega_{\mathrm{m}0}}\tilde{R}_\mathrm{s}\end{aligned} \tag{32b}$$

Using the Routh–Hurwitz stability criterion, the stability conditions are

$$\gamma_0\boldsymbol{k}_0^\mathrm{T}\left(\alpha_0\mathbf{J} + \omega_{\mathrm{m}0}\mathbf{I}\right)\boldsymbol{i}_{\mathrm{s}0} < 0 \tag{33a}$$

$$\gamma_0\frac{\boldsymbol{k}_0^\mathrm{T}\left(\alpha_0\mathbf{I} - \omega_{\mathrm{m}0}\mathbf{J}\right)\boldsymbol{i}_{\mathrm{s}0}}{\omega_{\mathrm{m}0}} > -\alpha_0 \tag{33b}$$

Acknowledgment

The authors wish to acknowledge the preliminary studies on this observer by Mr. Simo Matikainen. The financial support given by the Academy of Finland and ABB Oy is gratefully acknowledged.

References

[1] B. Nahid-Mobarakeh, F. Meibody-Tabar, and F.-M. Sargos, "Mechanical sensorless control of PMSM with online estimation of stator resistance," *IEEE Trans. Ind. Appl.*, vol. 40, no. 2, pp. 457–471, Mar./Apr. 2004.

[2] M. Jansson, L. Harnefors, O. Wallmark, and M. Leksell, "Synchronization at startup and stable rotation reversal of sensorless nonsalient PMSM drives," *IEEE Trans. Ind. Electron.*, vol. 53, no. 2, pp. 379–387, Apr. 2006.

[3] S. Koonlaboon and S. Sangwongwanich, "Sensorless control of interior permanent-magnet synchronous motors based on a fictitious permanent-magnet flux model," in *Conf. Rec. IEEE-IAS Annu. Meeting*, Hong Kong, Oct. 2005, pp. 311–318.

[4] S. Sangwongwanich, S. Suwankawin, S. Po-ngam, and S. Koonlaboon, "A unified speed estimation design framework for sensorless ac motor drives based on positive-real property," in *Proc. PCC-Nagoya'07*, Nagoya, Japan, Apr. 2007, pp. 1111–1118.

[5] S. D. Wilson, G. W. Jewell, and P. G. Stewart, "Resistance estimation for temperature determination in PMSMs through signal injection," in *Proc. IEEE IEMDC'05*, San Antonio, TX, May 2005, pp. 735–740.

[6] K.-W. Lee, D.-H. Jung, and I.-J. Ha, "An online identification method for both stator resistance and back-EMF coefficient of PMSMs without rotational transducers," *IEEE Trans. Ind. Electron.*, vol. 51, no. 2, pp. 507–510, Apr. 2004.

[7] K.-H. Kim, S.-K. Chung, G.-W. Moon, I.-C. Baik, and M.-J. Youn, "Parameter estimation and control for permanent magnet synchronous motor drive using model reference adaptive technique," in *Proc. IEEE IECON'95*, vol. 1, Orlando, FL, Nov. 1995, pp. 387–392.

[8] M. Hinkkanen, T. Tuovinen, L. Harnefors, and J. Luomi, "A reduced-order position observer with stator-resistance adaptation for PMSM drives," in *Proc. IEEE ISIE 2010*, Bari, Italy, July 2010, in press.

[9] L. Harnefors, M. Jansson, R. Ottersten, and K. Pietiläinen, "Unified sensorless vector control of synchronous and induction motors," *IEEE Trans. Ind. Electron.*, vol. 50, no. 1, pp. 153–160, Feb. 2003.

[10] L. Harnefors, "Design and analysis of general rotor-flux-oriented vector control systems," *IEEE Trans. Ind. Electron.*, vol. 48, no. 2, pp. 383–390, Apr. 2001.